Available online at www.sciencedirect.com
SCIENCE DIRECT
Journal of Catalysis 235 (2005) 1–9
JOURNAL OF CATALYSIS
www.elsevier.com/locate/jcat

Selective hydrogenation of crotonaldehyde on $Pt/ZnCl_2/SiO_2$ catalysts

Fatima Ammari [a], Candida Milone [b], Raymonde Touroude [a,*]

[a] *LMSPC, UMR 7515 du CNRS, ECPM, ULP, 2, rue Becquerel, 67087 Strasbourg cedex 2, France*
[b] *Dipartimento di Chimica Industriale e Ingegneria dei Materiali, Universita di Messina, Salita Sperone 31, I-98166 Messina, Italy*

Received 9 May 2005; revised 6 July 2005; accepted 8 July 2005

Available online 18 August 2005

Abstract

5 wt% Pt deposited on two different supports made of 3 and 1/6 equivalent monolayers of $ZnCl_2$ deposited on silica (termed Pt30 and Pt2) were prepared and tested in the selective hydrogenation of crotonaldehyde. Pt-based catalysts were prepared starting from tetraammine platinum nitrate as a metallic salt precursor. These catalysts showed very different catalytic behaviors in terms of the activity and the selectivity during time on stream. Pt2 was more active than Pt30 but less selective toward the formation of crotyl alcohol. On the Pt30 catalyst, the selectivity to the formation of crotyl alcohol increased with the reduction temperature, whereas the activity did not change significantly. When the catalyst was reduced at 400 °C, the selectivity to crotyl alcohol was >80%. It behaved similarly to Pt/ZnO catalysts prepared from hexachloroplatinic acid precursor [F. Ammari, J. Lamotte, R. Touroude, J. Catal. 221 (2004) 32]. In contrast, the Pt2 sample showed a decrease in the selectivity to crotyl alcohol and an increase in the activity with increasing reduction temperature. The catalysts were extensively characterized by BET, X-ray diffraction, X-ray photoelectron spectroscopy, transmission electron microscopy, and Fourier transform infrared pyridine adsorption. The higher selectivity of Pt30 is explained by a synergetic effect of Zn and chlorine. The greater amount of chlorine present on the catalyst surface led to an increase in the Lewis acidity of the support; moreover, the formation of PtZn alloy was observed. In agreement with our previous findings, we propose that modification of the electronic properties of platinum both from alloying to Zn and from the Lewis acidity of the support changes the adsorption mode of crotonaldehyde by favoring the binding of terminal oxygen of the molecule to the electronically modified platinum atoms.

Keywords: Selective crotonaldehyde hydrogenation; Chlorine effects; High crotyl alcohol selectivity; PtZn alloy; Lewis acidity; $ZnCl_2/SiO_2$ catalyst support; Platinum catalysts

1. Introduction

The selective hydrogenation of α,β-unsaturated aldehydes to produce unsaturated alcohols has been attracting much interest in fundamental research in catalysis [1]. The hydrogenation of the C=O bond over the C=C bond is not favored for thermodynamic and kinetic reasons. Thermodynamics favor the hydrogenation of C=C over C=O by about 10 kcal/mol [2]; moreover, the reactivity of the C=C group in hydrogenation is higher than that of the C=O group.

The platinum-based catalysts are used mostly for crotonaldehyde hydrogenation, and various factors controlling the intramolecular selectivity have been studied. An increase in the selectivity toward unsaturated alcohol was obtained by adding promoters [3–5], by using bimetallic catalysts [6,7] and by varying the nature of supports. In general, monometallic catalysts supported on Al_2O_3 or SiO_2 led mostly to the formation of the saturated aldehyde [2,4,6,8]. However, an increase in the selectivity of unsaturated alcohol was observed using TiO_2 as a support, which was able to create strong metal–support interactions (SMSIs) when Pt/TiO_2 was reduced at high temperature [2,9]. The widely accepted mechanism to explain the enhancement of selectivity towards the formation of unsaturated alcohol on catalysts under an SMSI state is the activation of the C=O bond on special active sites created by the partially reduced support (TiO_x) covering Pt particles [2]. Particle size is also consid-

* Corresponding author.
E-mail address: touroude@chimie.u-strasbg.fr (R. Touroude).

0021-9517/$ – see front matter
doi:10.1016/j.jcat.2005.07.008

ered to affect the catalytic properties and product selectivity. English et al. [10] suggested that on Pt/SiO_2 and Pt/TiO_2 catalysts, crotyl alcohol formation was favored on large Pt particles.

Recently we studied the hydrogenation of crotonaldehyde on Pt/ZnO catalysts [11,12]. Pt catalysts prepared from platinum chloride precursor were found to be more selective toward the hydrogenation of C=O than analogous catalysts prepared from tetraammine platinum nitrate. On the ex-chloride catalyst, 90% crotyl alcohol selectivity was reached. From this study clearly indicated that zinc and chlorine exert synergetic effects to increase crotyl alcohol selectivity. The Lewis acidity of the support, reinforced by chlorine and the formation of PtZn alloy, were found to be the key factors leading to high crotyl alcohol yield. It was proposed that modifying the electronic properties of platinum by alloying to Zn and by the Lewis acidity of the support changes the adsorption mode of crotonaldehyde by favoring the binding of the terminal oxygen of the molecule to the electronically modified platinum atoms [12].

The promoting effect of Zn or chloride on the selective hydrogenation of α,β-unsaturated aldehydes has been reported previously. On Pt/TiO_2 and Pt/CeO_2–SiO_2, beneficial effects of Zn addition were found at high reduction temperature [13–15], but in these studies the maximum crotyl alcohol selectivity never exceeded 40%. Nitta et al. [16] found that in α,β-unsaturated aldehyde hydrogenation, the presence of chlorine in cobalt catalysts enhanced the C=O hydrogenation selectivity. Tuley and Adams [17] found that unsupported Pt catalysts were promoted by Zn(II) and Fe(III) chlorides in liquid phase hydrogenation of cinnamaldehyde to cinnamyl alcohol.

Taking into account the results obtained on the ex-chloride platinum supported on ZnO [11,12], it appeared to be of great interest to investigate the behavior of catalysts prepared by dispersing Pt on a support containing $ZnCl_2$ deposited on SiO_2. In principle, these supports should contain all of the ingredients necessary to achieve high selectivity toward the formation of crotyl alcohol in the hydrogenation of crotonaldehyde. Indeed, we will have the presence of Zn and chloride, which are beneficial for the enhancement of the selectivity to unsaturated alcohol, as well as a strong Lewis acidity. Indeed, $ZnCl_2$ supported on SiO_2 has been used for the selective isomerization of citronellal to isopulegol, which is the first step in the synthesis of menthol from citronellal, a reaction catalyzed by Lewis acid sites [18].

These new systems were characterized by different methods: atomic absorption spectroscopy (AAS), nitrogen adsorption (BET), X-ray photoelectron spectroscopy (XPS), temperature-programmed reduction (TPR), Fourier transform infrared spectroscopy (FTIR), and transmission electronic microscopy (TEM). A comparison of the catalytic behavior in the hydogenation of crotonaldehyde of Pt supported on $ZnCl_2/SiO_2$ with that observed on Pt/ZnO catalysts [11,12] is presented.

2. Experimental

2.1. Catalyst preparation

$ZnCl_2/SiO_2$ supports were prepared by impregnation of SiO_2 (Grace Davison 432; surface area 330 m^2/g) with a methanolic solution of $ZnCl_2$ containing the proper amount of $ZnCl_2$, 38/62 and 4/96 weight ratio $ZnCl_2/SiO_2$, equivalent to 3 and 1/6 monolayers of $ZnCl_2$ onto SiO_2. The supports were dried overnight at 120 °C and then calcined in air at 350 °C for 2 h.

Two catalysts containing 5 wt% Pt, termed Pt30 and Pt2, were prepared by impregnating the high and low $ZnCl_2$-loaded supports, respectively, with an aqueous solution of $Pt(NH_3)_4(NO_3)_2$. The water was slowly evaporated, and the samples were dried overnight at 120 °C, calcined in air at 350 °C for 4 h, and reduced at different temperatures for 4 h.

2.2. Crotonaldehyde hydrogenation

Hydrogenation of crotonaldehyde was carried out at 80 °C at atmospheric pressure using a glass flow reactor as described previously [11]. The crotonaldehyde (100–500 µl) was introduced in a trap maintained at different temperatures depending on the desired partial pressure. The reaction products—crotyl alcohol, butanal, butanol, hydrocarbons, and other byproducts (called A and B herein)—were analyzed by gas chromatography (GC) with a DB-Wax column (30 m long, 0.53 mm i.d.; JW Scientific), working at 85 °C using a flame ionization detector. The byproducts and hydrocarbons were identified using a Chromapack column (50 m long, 0.32 mm i.d.; CP-Wax-58CB) connected to a mass spectrometer (Fisons).

2.3. Catalyst characterization

The platinum catalysts and parent supports were characterized by different methods. TEM analyses were performed on a TOPCON 002B electron microscope, operating at 200 kV, with a point-to-point resolution of 0.18 nm in high-resolution TEM (HRTEM) mode. Some catalyst grains, taken after the different catalytic pretreatments performed in the catalytic apparatus, were ground and diluted in an ethanol solution. One drop of this solution, previously dispersed in an ultrasonic tank, was deposited onto a Cu grid coated by a holey carbon film and dried in air. Various regions of the grid were observed, and the particle sizes were measured from the observation of 250–500 particles. The following formula was used to calculate the mean surface diameter: $d_s = \sum n_i d_i^3 / \sum n_i d_i^2$, where n_i is the number of particles of d_i diameter. Nanoprobe X-ray fluorescence was also used to check the nature of elements present in the selected area ($d = 14$ nm). The infrared measurements were performed at IMSRA (Caen, France) with an infrared quartz cell, with in situ catalyst treatments carried out at the desired temperature. The samples, prereduced at 673 K, were

evacuated at 473 K, and the pulses of pyridine were introduced at room temperature. The spectra were recorded using a NICOLET Magna 550 spectrometer, in the frequency region 1400–1700 cm^{-1}. The precision of the measurement of the frequency of the ν_{8a} pyridine band can be estimated at ± 0.1 cm^{-1}. The amounts of chlorine, zinc and platinum contained in the catalysts were measured by AAS performed at CNRS (Vernaison, France). BET surface areas were obtained using a Coulter SA3100 machine. The phase compositions of the samples were determined from XRD analyses performed on a Siemens D 5000 polycristalline diffractometer using Cu-K_α radiation. XPS measurements were carried out with a VG ESCA III machine. X-rays were generated with a magnesium or an aluminum anode (Mg-$K_\alpha = 1253.6$ and Al-$K_\alpha = 1486.6$ eV, 220 W), without a monochromator. The spectra were recorded at a pass energy of 20 eV. Due to the overlap between the Cl(2s) XPS line and Auger LMM Zn lines when using a Mg anode, the Auger Zn lines were recorded using an Al anode. The treatment of samples was done at atmospheric pressure in a preparation chamber attached directly to the analysis chamber. During analysis, the pressure in the chamber was about 10^{-9} Torr. The binding energy of Pt(4f), the Lorentzian half-width (γ Pt(4f)), and atomic ratios of Pt/Si, Zn/Si, Cl/Si, Cl/Zn, and Pt/Zn were deduced from the spectra obtained after curve fitting [11]. Because the charges were not compensated for, all of the spectra were recalibrated in terms of binding energies (BEs) using Si(2p) at 102.8 eV as the BE reference. After deconvolution, the Si(2p) peak shifted to 102.3 eV, which was taken as the reference for Pt($4f_{7/2}$) BE in the 60–110 eV region, which contains Pt(4f), Zn(3p), and Si(2p) peaks. The element intensity ratios were calculated from the peak surface ratio measurements, corrected by differences in escape depths (using a root squared approximation), and in cross-sections using Scofield data [19].

3. Results

3.1. Characterization

3.1.1. Chemical analysis

Table 1 gives the platinum, zinc, and chlorine amounts (wt%), of the Pt30 and Pt2 catalysts and of the parent supports analyzed by AAS. After calcination, both supports did not retain the initial stoichiometry of $ZnCl_2$, because the atomic ratios Zn/Cl were close to 1. The percentages of zinc and chlorine remained constant after platinum impregnation and calcination at 350 °C. These quantities were not affected by the reduction treatment at temperature <400 °C. After reduction at 400 and 500 °C, significant decreases in Zn% and, to a much greater extent, Cl% were observed on Pt30, whereas on Pt2, these decreases were hardly significant. Under a hydrogen stream, $ZnCl_2$ likely partially evaporated, with the remaining quantity decomposing to zinc and chlorine, which remained on the catalyst. After calcination

Table 1
Chemical analysis by AAS in wt% (knowing that $M_{Zn} = 65.9$ g; $M_{Cl} = 35.5$ g; $M_{Pt} = 195.1$ g) and particle sizes (D_s in nm) by TEM and XRD analysis

Treatment	Calcination	Reduction (°C)			
	350	200	300	400	500
(38/62)$ZnCl_2/SiO_2$ support					
(AAS) Zn (%)	17.8				
(AAS) Cl (%)	8.9				
Pt30 catalyst					
(AAS) Pt (%)	5.3	5.3	5.3	5.3	5.3
(AAS) Zn (%)	17.8	–[a]	19.4	13.2	10.4
(AAS) Cl (%)	8.9	9.6	8.3	1.5	0.6
(TEM (XRD)) D_s (nm)		7.6 (9.8)[b]		9.4	11 (11.3)[b]
(4/96)$ZnCl_2/SiO_2$ support					
(AAS) Zn (%)	1.9				
(AAS) Cl (%)	1.2				
Pt2 catalyst					
(AAS) Pt (%)	5.1	5.1	5.1	5.1	5.1
(AAS) Zn (%)	1.9	–[a]	1.9	1.7	1.67
(AAS) Cl (%)	1.2	–[a]	0.8	–[a]	0.72
(TEM (XRD)) D_s (nm)			4.4		4.3

[a] Non determined.
[b] ( ) Values deduced from XRD measurements.

Table 2
Surface area measured by BET on Pt30 and Pt2 catalysts and on the corresponding supports

	Support	Catalyst				
		Calc. 350 °C	Red. 200 °C	Red. 300 °C	Red. 350 °C	Red. 500 °C
Pt30	167.4	136.3	143.2	167.8		214.4
Pt2	295.3	276.9		248.6	200.2	

treatment, the platinum percentages were very close to 5%, which was the initially desired value on both the Pt30 and Pt2 catalysts.

3.1.2. BET analysis

The specific surface areas obtained on the Pt30 and Pt2 catalysts and the parent supports are reported in Table 2. Pt30, which contained higher quantities of $ZnCl_2$, and its corresponding support, had a lower specific surface than Pt2, demonstrating that $ZnCl_2$ blocked the silica pores. On Pt30, the surface area increased when the reduction temperature increased. Because decreased Zn and Cl percentages with increasing reduction temperature were observed by AAS on this catalyst, it can be concluded that $ZnCl_2$ evaporated and unblocked the silica pores. In contrast, on Pt2, the surface area, which was initially higher, decreased with increasing reduction temperature. The surface area of Pt2 reduced at 350 °C was close to that of Pt30 reduced at 500 °C. The decreased specific surface area of Pt2 after reduction at high temperature cannot be ascribed to a collapse of the SiO_2 pores, because then similar behavior should also be observed on Pt30, but instead, an increase in surface area with increas-

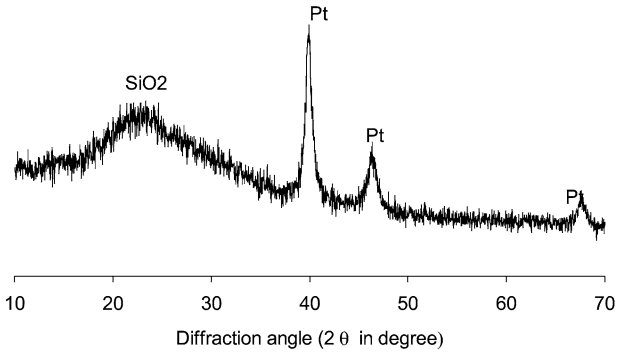

Fig. 1. XRD of Pt30 calcined at 350 °C.

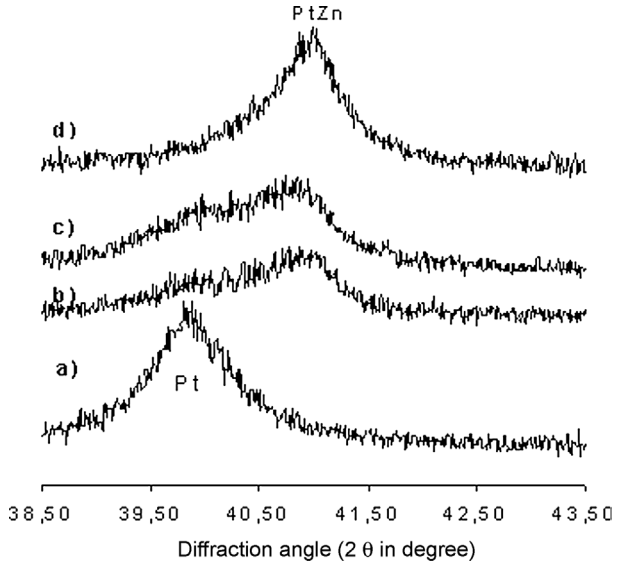

Fig. 2. XRD of Pt30 reduced at different temperatures: (a) 200, (b) 300, (c) 400, and (d) 500 °C.

ing reduction temperature is observed on this catalyst. It can be argued that the decreased surface area on Pt2 is due to silica particle rearrangement; we discuss this point later in this paper.

3.1.3. XRD analysis

Fig. 1 shows the XRD spectra of Pt30 calcined at 350 °C in the range $2\theta = 10°$–$70°$. Fig. 2 reports the XRD spectra of Pt30 reduced at different temperatures, in the range $2\theta = 38.5°$–$43.5°$. For Pt2, no diffraction lines could be discerned regardless the reduction temperature, because of the small size of the metal particles. For Pt30, after calcination at 350 °C, the spectra showed a wide line between 15° and 38°, characteristic of silica (Fig. 1). Three well-defined lines characteristic of metallic platinum (JCPS 4-0802), with the main line, Pt(111), at 39.75° and two less intense lines, Pt(200) and Pt(220), at 46.3° and 67.8°, respectively, were also seen. These results demonstrate that platinum particles were already in a reduced state after calcination. Metallic platinum was still present on Pt30 reduced at 200 °C (Fig. 2). Increasing the reduction temperature from 300 to 400 °C produced the superposition of Pt and Pt–Zn alloy phases [JCPS 6-0604, PtZn(111) at 40.79°], and after reduction at 500 °C, the PtZn alloy was the quasi-unique phase. The Pt line after reduction at 200 °C and the PtZn line after reduction at 500 °C were of similar width. The average particle sizes calculated from Scherrer equation are reported in Table 1.

3.1.4. XPS results

Table 3 gives the BE, Lorentzian half-width (γ) of Pt ($4f_{7/2}$), atomic ratios of Pt/Si, Zn/Si, Cl/Si, Cl/Zn and Pt/Zn for Pt30 treated in situ the XPS apparatus at different temperatures. Fig. 3 shows the spectra in the 65–80 eV region corresponding to the Pt(4f) lines. For Pt2, the weakness of the Zn signals did not allow to get accurate information from the XPS analysis. For Pt30, the changes observed on the Pt($4f_{7/2}$) BE (70.5 ± 0.2 eV) were not significant at the different reduction temperatures, evidencing the metallic character of Pt. A small BE increase was observed after calcination due to the chemisorption of oxygen atoms, but platinum was not in oxide form. This result is in agreement with the observations of the XRD analysis (Fig. 1). The Lorentzian half-width γ(Pt($4f_{7/2}$) decreased significantly, from 0.91 to 0.59, with an increase in reduction temperature from 200 to 500 °C, in agreement with the transformation of Pt to PtZn phases as already observed in Pt/ZnO catalysts [11]. The atomic ratios of Zn/Si and Cl/Si did not change when the reduction temperature increased from 200 to 300 °C but decreased significantly at 500 °C, with a much more pronounced effect for chlorine (Table 3). These results are in agreement with that observed in the bulk analysis (AAS; Table 1). It should be pointed out that the amounts

Table 3
XPS results on Pt30 after reduction at different temperatures

	Pt($4f_{7/2}$)		Atomic ratios				
	BE (eV)	γ	(Pt/Si) × 100	Zn/Si	Cl/Si	Cl/Zn	Pt/Zn
Initial			2.8[a]	0.28[a]	0.55[a]	2[a]	0.1[a]
Calc. 350 °C	70.9	1.0	1.5 (2.4)[b]	0.33 (0.24)[b]	0.27 (0.22)[b]	0.87 (0.92)[b]	0.045 (0.1)[b]
Red. 200 °C	70.7	0.91	0.96	0.35	0.35	1.0	0.027
Red. 300 °C	70.4	0.67	0.76 (2.4)[b]	0.34 (0.26)[b]	0.32 (0.21)[b]	0.92 (0.81)[b]	0.022 (0.09) [b]
Red. 500 °C	70.6	0.59	0.75 (2.0)[b]	0.18 (0.11)[b]	0.07 (0.012)[b]	0.4 (0.11)[b]	0.042 (0.18) [b]

[a] Initial values calculated from Pt30 prepared with the following weight percentages: 5.32% Pt, 36.43% $ZnCl_2$, 58.25% SiO_2.
[b] ( ) Values calculated from AAS results (atomic ratios in volume).

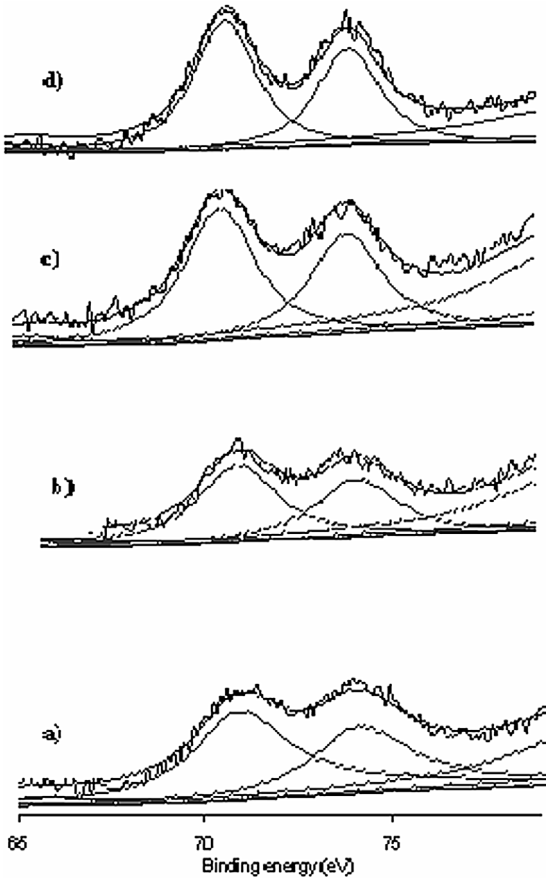

Fig. 3. Pt (4f) XPS lines of Pt30 treated at different temperatures: (a) calcined at 350 °C, (b) reduced at 200 °C, (c) reduced at 300 °C, reduced at 500 °C.

of Zn and chlorine determined by XPS was always greater than those calculated from AAS, demonstrating that Zn and Cl species were localized mainly on the silica surface. This also can be proven by analyzing the Zn(2p)/Zn(3p) intensity ratios, the two XPS lines Zn(2p) and Zn(3p) generated by photoelectrons of two different kinetic energies (KEs), 464.8 and 1398.3 eV, respectively. This ratio should be 1 if Zn is distributed equally in the surface and in the bulk, as was verified in our reference samples, ZnO, $ZnCl_2$, and Pt/ZnO [11,12]. On Pt30, this ratio was 3. As explained previously [20], the overintensity of the low-KE XPS line is proof that the element is localized at the surface.

Measured by XPS or AAS, the Cl/Zn atomic ratios were similar and close to 1, except at 500 °C, where Cl became half of the Zn atoms in surface.

The Zn LMM Auger spectra were also recorded because, in contrast to Zn(2p) or Zn(3p) BE, which were found to be similar for several reference Zn-containing compounds, the Auger Zn KE was found to differ in several reference compounds, including metal Zn, ZnO, and $ZnCl_2$ [21–23]. Fig. 4 presents the Zn Auger spectra obtained on Pt30 calcined at 350 °C and on Pt30 reduced at 200 and 300 °C and compares these results with those obtained on a 1% Pt/ZnO ex-chloride system [24]. The KEs of Zn LMM Auger spectra are summarized in Table 4. Taking into account that $Zn(2p_{3/2})$ BE was localized at 1021.8 eV on all of the samples, the support alone (38/62) $ZnCl_2/SiO_2$ and Pt30 catalyst treated at different temperatures had a significantly lower KE (986.8 ± 0.1 eV) than 1% Pt/ZnO (988.3 ± 0.2 eV). This lower value corresponds to that reported by Fiermans et al. [22] for $ZnCl_2$ species. From these results, it is clear that there was no formation of ZnO species at the surface of Pt30 after calcination and reduction treatments. However, based on the stoichiometry obtained from XPS and AAS (Zn/Cl close to 1), the presence of $ZnCl_2$ is unlikely. It is also noteworthy that the parts of the zinc atoms that were alloyed with Pt to form PtZn were too small to influence the XPS or Auger Zn signals (initially, the catalyst contained 10 times less Pt than Zn atoms). Therefore, we conclude that during thermal treatment of the Pt30 catalyst, $ZnCl_2$ decomposes, and no ZnO formation occurs. Based on the Zn LMM Auger results, it can be argued that –O–Zn–Cl species graphed on the silica surface are formed. For the catalyst reduced at a

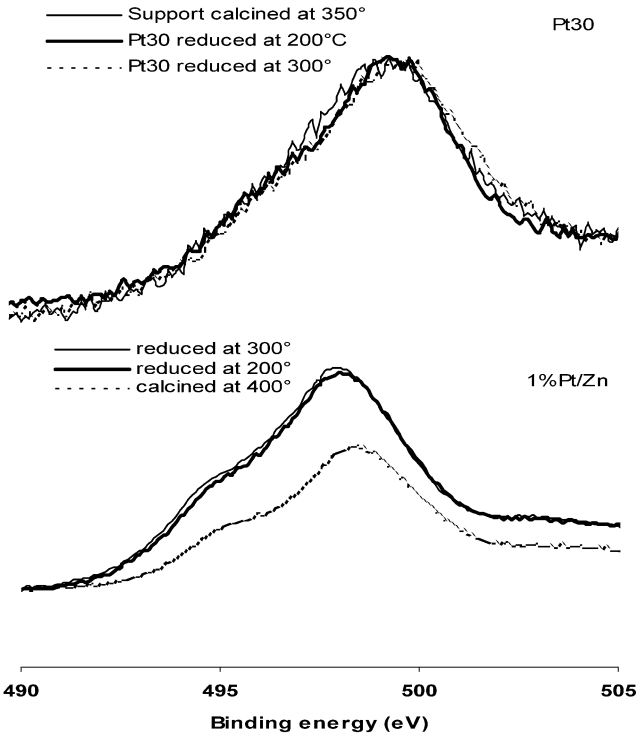

Fig. 4. Zn LMM Auger lines (using Al-K_α source) of Pt30 and of 1% Pt/ZnO ex-chloride [24].

Table 4
Zn LMM Auger peak KE obtained on 1% Pt/ZnO [24], (38/62)$ZnCl_2/SiO_2$ and Pt30

	1% Pt/ZnO	(38/62)$ZnCl_2/SiO_2$	Pt30
Calc. 400 °C	988.1	986.8	
Red. 200 °C	988.4		986.9
Red. 300 °C	988.5		986.7

$Zn(2p_{3/2})$ BE = 1021.8 eV.

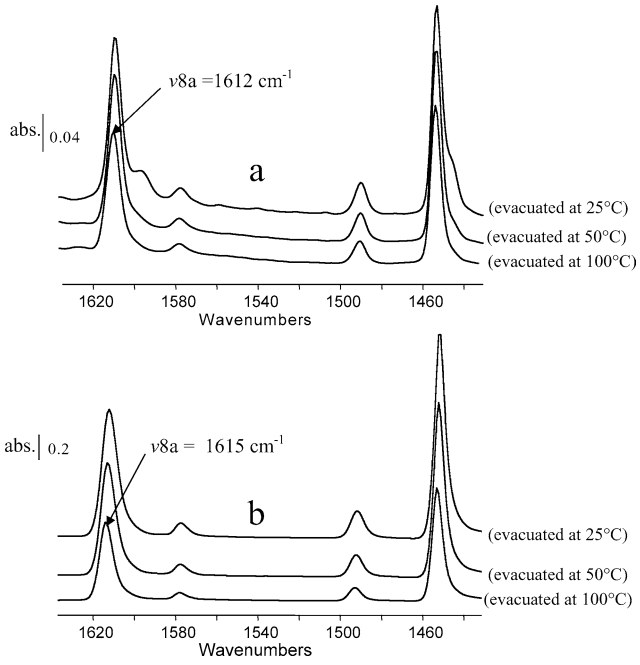

Fig. 5. FTIR analyses, pyridine adsorption spectra on (a) Pt2 reduced at 400 °C and (b) Pt30, reduced at 400 °C.

temperature >200 °C, a small amount of Zn is alloyed with platinum.

3.1.5. TEM results

Table 1 reports the diameters of Pt particles of Pt30 and Pt2 obtained by TEM and compares these with those obtained by XRD analyses. On Pt30, the particle sizes given by both methods were in acceptable agreement. At all reduction temperatures, the platinum particles were smaller on Pt2 than on Pt30. The increase in reduction temperature from 200 to 500 °C led to an increased particle size on Pt30, but not on Pt2.

3.1.6. FTIR results

Pyridine adsorption on Pt2 and Pt30 was studied by FTIR after in situ reduction at 400 °C (Fig. 5). No band localized in the 1540–1550 cm^{-1} frequency range, characteristic of pyridinium ion revealing the Brønsted acidic character of the surface, was observed on either catalyst [25]. The two main bands were localized around 1450 and 1610 cm^{-1}. These bands are characteristic of the Lewis acidity of the surface; they correspond to the ν_{8a} and ν_{19b} vibration modes of the coordinately bonded pyridine. The ν_{8a} vibration is sensitive to the mode of adsorption and indicates the nature and strength of the Lewis acidity, whereas the ν_{19b} vibration is characteristic of the number of sites existing on the catalyst surface [26]. Their counterparts, ν_{8b} and ν_{19a} localized at 1580 and 1490 cm^{-1}, respectively, are not sensitive to acidity strength. On the Pt30 catalyst (Fig. 5b) two bands localized precisely at 1615 and 1454 cm^{-1} were observed after pyridine adsorption and evacuation treatment at different temperatures. The position of the ν_{8a} band at

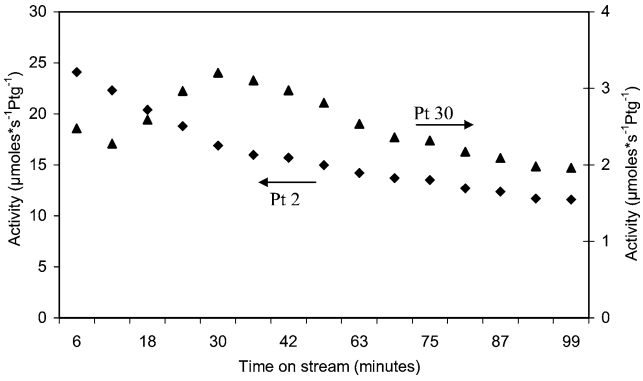

Fig. 6. Activity as a function of time on stream on Pt30 reduced at 400 °C (▲) and on Pt2 reduced at 200 °C (◆).

1615 cm^{-1} and the absence of desorption with increasing evacuation temperature indicated the presence of strong acidity on this catalyst. On Pt2 (Fig. 5a), the ν_{8a} band was observed at 1612 cm^{-1}, slightly (but significantly) lower than in Pt30 [27]. The intensity of ν_{19b} band was lower than the one observed on Pt30. These two observations showed that the Lewis acidic sites were more numerous and with a stronger acidity on Pt30 than on Pt2. In addition to these two main bands, characteristic of the Lewis acidity, an additional band at 1600 cm^{-1} was present after pyridine adsorption on Pt2, but disappeared after evacuation treatment at 50 °C. This band corresponds to hydrogen-bonded pyridine [12], indicating the existence of OH groups on the catalyst surface, which did not exist on Pt30.

3.2. Crotonaldehyde hydrogenation

It is generally observed that when hydrogenation reactions are performed in a flow catalytic system, the distribution of the products (unreacted product and reaction products) changes from the beginning to the end of the time on stream (TOS), with an initial regime usually preceding the steady-state regime [28,29]. The length of this initial period depends on the space velocity of the reactant (F/ω), the adsorption properties of the support toward the reactant and the reaction products, and catalyst stability. The Pt2 and Pt30 catalysts showed two different evolutions of the total activity as a function of TOS as presented in Fig. 6. For Pt2, an initial deactivation was observed; for Pt30, increased activity was observed during the first 30 min that then decreased with TOS. But on both catalysts, a quasi–steady-state regime was established after a certain time. The catalytic behavior expressed in terms of activity and product distributions in the steady-state regime of Pt30 and Pt2 are reported in Table 5. The reactions were performed at 80 °C under 8 Torr crotonaldehyde pressure and 752 Torr hydrogen pressure. Regarding the activities, two main observations can be made: (i) Pt2 was much more active than Pt30, and (ii) the increase in reduction temperature from 200 to 500 °C led to an increase in activity that was much more pronounced on Pt2 than on Pt30. Finally, at a reduction temperature of 500 °C,

Table 5
Hydrogenation of crotonaldehyde on Pt30 and Pt2 reduced at different temperatures

	Pt30				Pt2			
Red. T (°C)	200	300	400	500	200	300	400	500
A (μmol/(s g_{Pt}))	1.5	2.1	1.7	3.5	13.4	37.5	74.9	360
Selectivity (%)								
(At conversion (%))	(3.1)	(4.3)	(4.3)	(7.1)	(8.5)	(7)	(15)	(33)
Hydrocarbons	6	4	2.7	1	0	0	0	0
A by-product	9	10	3.8	1	0	0	0	0
Butanal	18	13	14.8	20	45.1	58.2	56.6	51.1
B by-product	12	14	6.8	3.5	0	0	0	0
Butanol	–	4	5.2	6.5	6.3	6.3	11.3	31.3
Crotyl alcohol	*55*	*55*	*67*	*68*	48	35.6	32.2	17.6
C=O/C=C[a]	*3.1*	*3.5*	*3.6*	*2.8*	1.1	0.6	0.6	0.6

[a] $C{=}O/C{=}C = (S_{\text{crotyl alcohol}} + S_{\text{butanol}})/(S_{\text{butanal}} + S_{\text{butanol}})$.

Pt2 was 100 times more active than Pt30. The product distributions expressed in terms of selectivity are reported for conversions usually <10%, to limit the effects due to the second hydrogenation step (butanol formation). Because of the high activity of Pt2 reduced at 400 and 500 °C, the product distributions were taken at 15 and 30% of conversion respectively. On Pt2, the selectivity to crotyl alcohol reached 48% after reduction at 200 °C and decreased with increasing reduction temperature. No hydrocarbon or byproduct formation was observed. On Pt30, in contrast, crotyl alcohol was the main reaction product, and the selectivity increased from 55 to 68% with increasing reduction temperature. The selectivity to butanal was less influenced by the reduction temperature, whereas the formation of hydrocarbons and A and B byproducts were observed. In particular, their selectivity decreased with increasing reduction temperature. Hydrocarbons and A and B byproducts, identified by GC-MS analyses, corresponded to C_4 hydrocarbons (mainly butadiene and small amounts of butenes and butane) and *cis* and *trans* crotyl chloride (1-chloro, but-2-ene), respectively. The formation of these byproducts had been also observed in the hydrogenation of crotonaldehyde on ex-chloride Pt/ZnO catalyst [12]. Butadiene and crotyl chloride are likely formed by secondary reactions of crotyl alcohol, dehydratation and replacement of OH by Cl, catalyzed by the acidic support, as discussed later in this paper. Butenes and butane are formed from hydrogenation of butadiene.

Fig. 7 reports product selectivity as a function of TOS for Pt30 reduced at 400 °C. During the first 30 min, corresponding to the activation period (see Fig. 6), butanal, A and B byproducts, and hydrocarbons decreased and crotyl alcohol and, to a lesser extent, butanol increased. We propose that in the earlier stage of reaction, before mass balance between the inproducts and outproducts is reached, the catalyst was very active in producing crotyl alcohol. Crotyl alcohol remained adsorbed on the catalyst (specially on the support) and reacted on the acidic support to be transformed into A and B byproducts, hydrocarbons, and butanal by isomerization and probably higher-molecular-weight products that re-

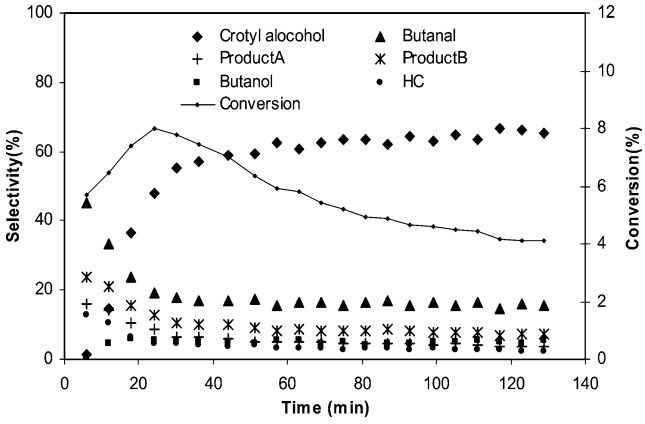

Fig. 7. Selectivity and conversion as a function of time on stream on Pt30 at 400 °C.

Table 6
Hydrogenation of crotonaldehyde on Pt30 reduced at 400 °C as a function of crotonaldehyde pressure and comparison with Pt/ZnO catalysts reduced at 400 °C

	Catalysts					
	Pt 30				5% Pt/ZnO [24]	1% Pt/ZnO [12]
Initial Cl (wt%)	1.5				0.7	0.5
Number of exp.	1	2	3	4	1	1
Total μl injected	100	80	160	280		
$P_{\text{crotonaldehyde}}$ (Torr)	8	8	13	21	8	8
A (μmol/(s g_{Pt})	1.7	1.5	4.5	6.5	2.8	8.4
Selectivity (%)						
(At conversion (%))	(3.2)	(4.2)	(5.6)	(4.7)	(7)	(11.7)
Hydrocarbon	2	3	1	0.2	3.1	0.8
A by-product	5	4	2	1	0.9	0.4
Butanal	16	17	15	13	10.1	12.9
B by-product	10	9	5	3	2.7	1
Butanol	1	1	1	1	1	1.8
Crotyl alcohol	66	66	76	*82*	*82.3*	*83.1*
C=O/C=C[a]	3.9	3.7	4.8	5.9	7.5	5.8
$\text{Yield}_{(HC + A + B)}$[b]	0.29	0.24	0.36	0.27		
$\text{Yield}_{\text{Butanal}}$[b]	0.27	0.26	0.68	0.85		
$\text{Yield}_{\text{Crotyl alcohol}}$[b]	1.12	0.99	3.42	5.3		

[a] $C{=}O/C{=}C = (S_{\text{crotyl alcohol}} + S_{\text{butanol}})/(S_{\text{butanal}} + S_{\text{butanol}})$.

[b] Expressed in μmol/(s g_{Pt}).

covered the surface and partially poisoned the support. After this period, crotyl alcohol formed by hydrogenation on the metallic part could no longer readsorb and react on the support; therefore, it desorbed, and the selectivity increased. But hydrocarbons and crotylchloride (A + B byproducts) were still produced, albeit at a lesser extent (Table 6). Repeating four times the experiments on the same catalytic charge, 100 mg of Pt 30 reduced at 400 °C, the selectivity to crotyl alcohol increased from one run to the next. Before each experiment, the catalyst was reduced for 4 h at 400 °C. Because of the lack of activity, the vapor pressure of crotonaldehyde was also increased. The activity and selectivity values for

each run are reported in Table 6; the total amount and the pressure of crotonaldehyde used in each experiment are indicated. Crotyl alcohol selectivity increased with an increased number of experiments on the same catalyst and increased vapor pressure to reach a value >80%. Moreover, the selectivity to hydrocarbons and A and B byproducts decreased. Therefore, in terms of product yields (activity*selectivity), the sum of hydrocarbon and crotyl chloride yields remained quasi-constant from one experiment to the other (0.3 ± 0.06) (Table 6), whereas the yields of hydrogenated products increased, in a more significant proportion for crotyl alcohol than for butanal.

4. Discussion

In selective hydrogenation of crotonaldehyde into unsaturated alcohol, $Pt/ZnCl_2/SiO_2$ catalysts showed the beneficial effects of zinc and chlorine on crotyl alcohol selectivity already observed in the ex-chloride Pt/ZnO catalyst [11,12]. Compared with Pt/SiO_2 [2,10], these catalysts were much more selective in carbonyl bond hydrogenation than in olefinic bond hydrogenation. However, Pt30 and Pt2 catalysts, prepared on supports containing different amounts of $ZnCl_2$, exhibit very different catalytic behaviors.

Pt2 was more active than Pt30, and an increase in the reduction temperature led to a huge increase in activity with a significant loss of selectivity to crotyl alcohol (Table 5). This evolution is going the opposite way to that expected due to a promoter effect [9–15]. On Pt2, a promoting effect of zinc and chlorine on the catalytic activity of Pt is observed when the catalyst is reduced at low temperature, leading to a rather high crotyl alcohol selectivity (48%). The observed decrease in crotyl alcohol selectivity with increasing reduction temperature means that the interactions between platinum and the promoters are gradually weakening. These interactions are quasi-destroyed after reduction at 500 °C to leave naked platinum particles, with increased activity accompanied by decreased selectivity observed. Nonetheless, it is noteworthy that the amount of zinc and chlorine on Pt2 did not change significantly with increasing reduction temperature (Table 1) while the surface area decreased simultaneously. The decrease in specific surface area of Pt2 after reduction at high temperature cannot be ascribed to a collapse of the SiO_2 pores, because if that were the case, then similar behavior should be observed on Pt30, but instead an increase in surface area with increasing reduction temperature is seen on this catalyst. It can be argued that the increased temperature of treatment caused Zn ions to penetrate into the silica support to form zinc silicate and then gave free the Pt particles. The formation of zinc silicate has been suggested in some preparations of $ZnCl_2/SiO_2$ [30] or ZnO/SiO_2 [31] systems. In our case, zinc silicate could not be characterized by XRD, because the amount formed was below the detection limit and/or because it was under an amorphous state.

Pt 30 was always less active but more selective to crotyl alcohol than Pt2, and the selectivity increased with increasing reduction temperature. The FTIR results obtained on catalysts reduced at 400 °C indicated the presence of Lewis acid sites on Pt30 and Pt2, with the number and the strength of those sites higher on Pt30 than on Pt2. The stronger Lewis acidity of the support of Pt30 was clearly revealed in the initial stage of the hydrogenation of crotonaldehyde, where a strong adsorption of crotyl alcohol on the support likely occurs; crotyl alcohol reacts on the acidic support to form butadiene and *cis*, *trans* crotyl chloride by dehydratation and OH–Cl exchange (Table 5). It is remarkable that the best results obtained on this catalyst were very similar to those obtained on Pt/ZnO catalysts prepared from hexachloroplatinic acid precursor (Table 6) [12,24]. A selectivity to crotyl alcohol >80% was never observed on Pt/ZnO catalysts prepared from platinum nitrate tetraamine precursor. On this catalyst, the crotyl alcohol selectivity never exceeded 50% [11,12, 24]. Therefore, we confirm that the presence of chlorine, provided from either the metallic precursor or the support, is essential to obtain a very high selectivity.

Looking at the Table 5, the optimized reduction temperature to obtain the higher crotyl alcohol selectivity and the higher C=O/C=C hydrogenation ratio on Pt30 was 400 °C. At lower reduction temperature, the content of byproducts was higher, and at 500 °C, butanal formation generally increased. Our research into the optimizing conditions on Pt30 reduced at 400 °C (Table 6) points up the beneficial effect of repeating the experiments in decreasing the formation of the secondary products, hydrocarbons, and crotyl chloride, and obtaining a greater crotyl alcohol selectivity. It should be noted that the amount of crotyl chloride decreased with a decreasing amount of chlorine in the catalyst. Indeed, comparing the reactivity of Pt30 catalysts reduced at different temperatures indicates a marked decrease in chlorine content with increasing reduction temperature (Table 1) and a simultaneous significant decrease in crotyl chloride selectivity (Table 5). Finally, the influence of chlorine in this catalytic system is very subtle; it clearly has a beneficial effect on the Lewis acidity of the support leading to an increase in the carbonyl bond hydrogenation, but the amount of chloride must be restricted within a certain limit to avoid the further conversion of crotyl alcohol into A and B byproducts. In addition, we note that a high level of chlorine had a negative effect on total activity. This was well demonstrated earlier by comparing the activity of 1% and 5% Pt/ZnO catalysts [12]; in the present study, this could explain the apparent positive order in crotyl alcohol formation versus crotonaldehyde pressure in the results given in Table 6. In fact, during one experiment the amount of chlorine in the catalyst decreased due to the formation of crotyl chloride; then, from one experiment to the next the chlorine content in the catalyst decreased while the activity increased.

In Pt30, the transformation of Pt to PtZn alloy with increasing reduction temperature was observed. On catalyst reduced at 400 °C, PtZn alloy was well characterized by XRD (Fig. 2) and XPS (Fig. 3). This catalyst showed the best performance toward carbonyl hydrogenation. However,

at 200 °C, where alloy formation was not observed by either XRD or XPS, the selectivity in the carbonyl bond hydrogenation was significantly high compared with that of Pt/SiO_2. This finding means that even at this low reduction temperature, zinc interacted with platinum and changed the intrinsic reactivity of platinum. As developed earlier [12], we have eliminated a possible bifunctional function of the catalyst in which hydrogen would dissociate on the metallic part (metal or alloy) and, through spillover, migrate on the support to hydrogenate crotonaldehyde adsorbed on the Lewis acidic sites, because Pd/ZnO catalysts prepared similarly to Pt/ZnO gave, for a similar activity, 100% C=C bond hydrogenation despite the acidic character of the support [24]. Generally, the best performances of the Pt/Zn/Cl-based catalysts were obtained after reduction at 400 °C, where PtZn alloy was observed. In theoretical and experimental studies on PtZn alloy, Rodriguez and Khun [32] found a decreased 5d population of Pt atoms in a PtZn structure. In our catalyst, such a decrease at the level of the metallic PtZn particle could be reinforced by the Lewis acidity of the support caused by the presence of chlorine (–O–Zn–Cl). The positively polarized metallic surface could orientate the adsorption of crotonaldehyde toward the C=O bond instead of the C=C bond and then enhance the formation of crotyl alcohol to the detriment of butanal in the hydrogenation reaction.

5. Conclusion

In this study, 5 wt% Pt deposited on two different supports made of 3 and 1/6 equivalent monolayers of $ZnCl_2$ deposited on silica (termed Pt30 and Pt2) were prepared and tested in the selective hydrogenation of crotonaldehyde. Pt-based catalysts were prepared starting from tetraammine platinum nitrate as a metallic salt precursor. These catalysts showed very different catalytic behavior in terms of activity and selectivity during TOS. Pt2 was more active than Pt30 but less selective toward the formation of crotyl alcohol. On Pt30, the selectivity to the formation of crotyl alcohol increased with increasing reduction temperature but the activity did not change significantly. When the catalyst was reduced at 400 °C, the selectivity to crotyl alcohol was >80%. It behaved similarly to Pt/ZnO catalysts prepared from hexachloroplatinic acid precursor [12]. In contrast, the Pt2 sample demonstrated decreased selectivity to crotyl alcohol and increased activity with increasing reduction temperature. It was proposed that when Pt2 is reduced at higher temperature, Zn interacts with silica rather than with Pt to probably form zinc silicate, leading to the decreased selectivity to crotyl alcohol. The higher selectivity of Pt30 has been explained by a synergetic effect of Zn and chlorine; the high amount of chlorine on the catalyst surface leads to increased Lewis acidity of the support, along with the formation of PtZn alloy. In agreement with our previous findings, we propose that modification of the electronic properties of platinum both by alloying to Zn and by the Lewis acidity of the support changes the adsorption mode of crotonaldehyde by favoring the binding of the terminal oxygen of the molecule to the electronically modified platinum atoms.

Acknowledgments

We are indebted to J. Lamotte from IMSRA in Caen (France) who has performed the FTIR analyses and helped us for their interpretation.

References

[1] P. Gallezot, D. Richard, Catal. Rev. Sci. Eng. 40 (1998) 81.
[2] M.A. Vannice, B. Sen, J. Catal. 115 (1989) 65.
[3] V. Ponec, Appl. Catal. A: Gen. 149 (1997) 27.
[4] J.L. Margitfalvi, A. Tompos, I. Kolosova, J. Valyon, J. Catal. 174 (1998) 246.
[5] S. Galvagno, G. Capannelli, G. Neri, A. Donato, R. Pietropaolo, J. Mol. Catal. 64 (1991) 237.
[6] M. English, V.S. Ranade, J.A. Lercher, J. Mol Catal. A: Chem. 121 (1997) 69.
[7] S. Galvagno, C. Milone, Catal. Lett. 17 (1993) 55.
[8] P. Claus, S. Schimpf, R. Schödel, P. Kraak, W. Mörke, D. Hönicke, Appl. Catal. A 165 (1997) 429.
[9] M.A. Vannice, Top. Catal. 4 (1997) 241–248.
[10] M. Englisch, A. Jentys, J.A. Lercher, J. Catal. 166 (1997) 25.
[11] M. Consonni, D. Jokic, D.Yu. Murzin, R. Touroude, J. Catal. 188 (1999) 165.
[12] F. Ammari, J. Lamotte, R. Touroude, J. Catal. 221 (2004) 32.
[13] J. Silvestre-Albero, F. Rodriguez-Reinoso, A. Sepulveda-Escribano, J. Catal. 210 (2002) 127.
[14] J. Silvestre-Albero, A. Sepulveda-Escribano, F. Rodriguez-Reinoso, J.A. Anderson, J. Catal. 223 (2004) 179.
[15] J. Silvestre-Albero, A. Sepulveda-Escribano, F. Rodriguez-Reinoso, J.A. Anderson, Phys. Chem. Chem. Phys. 5 (2003) 208.
[16] Y. Nitta, Y. Hiramatsu, T. Imanaka, J. Catal. 126 (1990) 235.
[17] W.F. Tuley, R. Adams, J. Am. Chem. Soc. 47 (1925) 3061.
[18] C. Milone, C. Gangemi, G. Neri, A. Pistone, S. Galvagno, Appl. Catal. A: Gen. 199 (2000) 239.
[19] J.H. Scofield, J. Electron. Spectrosc. Relat. Phenom. 8 (1976) 129.
[20] S.M. Davis, J. Catal. 117 (1989) 432.
[21] C.D. Wagner, W.M. Riggs, L.E. Davis, J.F. Moulder, G.E. Muilenberg, Handbook of X-Ray Spectroscopy, Perkin–Elmer Corporation, Eden Prairie, MN, 1979.
[22] L. Fiermans, R. Hoogewijs, J. Vennik, Surf. Sci. 47 (1975) 1.
[23] B.E. Green, C.S. Sass, L.T. Germinario, P.S. Wehner, B.L. Gustafson, J. Catal. 140 (1993) 406.
[24] F. Ammari, Thesis, Strasbourg, 2002.
[25] E.P. Parry, J. Catal. 2 (1963) 371.
[26] G. Berhault, M. Lacroix, M. Breysse, F. Maugé, J.-C. Lavalley, H. Nie, L. Qu, J. Catal. 178 (1998) 555.
[27] G. Busca, Phys. Chem. Chem. Phys. 1 (1999) 723.
[28] K. Tamaru, Dynamic Heterogeneous Catalysis, Academic Press, New York, 1978.
[29] J.B. Butt, Reaction Kinetics and Reactor Design, Dekker, New York, 2000.
[30] C. Chouillet, F. Villain, M. Kermarec, H. Lauron-Pernot, C. Louis, J. Phys. Chem. B 107 (2003) 3565.
[31] T. Sumiyoshi, K. Tanabe, H. Hattori, Bul. Chem. Soc. Jpn. 17 (1975) 65.
[32] J.A. Rodriguez, M. Kuhn, J. Chem. Phys. 102 (1995) 4279.